



# Fine mapping of genes controlling pigment accumulation in oilseed rape (*Brassica napus* L.)

Daozong Chen · Qingdong Jin · Jianming Pan · Yi Liu · Yijia Tang · Yanrong E · Linshan Xu · Taihua Yang · Jie Qiu · Xiaodi Chen · Jing Wang · Deping Gong · Xianhong Ge · Zaiyun Li · Cheng Cui

Received: 6 October 2022 / Accepted: 22 February 2023 / Published online: 9 March 2023  
© The Author(s), under exclusive licence to Springer Nature B.V. 2023

**Abstract** Purple/red appearance is one of the common phenotypic variations in leaves, stems, and siliques of oilseed rape (*Brassica napus* L.) but very

---

Daozong Chen and Qingdong Jin contributed equally to this work.

## Key message

We successfully fine mapped two genes controlling pigment accumulation in stems and flowers, respectively, in oilseed rape. Both candidate genes, *BnaPAP2.C6a* and *BnaPAP2.A7b*, belong to the R2R3-MYB gene family, were further determined according to the gene expression and allelic sequence comparison.

---

**Supplementary Information** The online version contains supplementary material available at <https://doi.org/10.1007/s11032-023-01365-5>.

---

D. Chen · Y. Liu  
College of Life Sciences, Ganzhou Key Laboratory of Greenhouse Vegetable, Gannan Normal University, Ganzhou 341000, China

Q. Jin · J. Pan · Y. Tang · Y. E · L. Xu · T. Yang · J. Qiu · X. Chen · J. Wang · X. Ge · Z. Li  
National Key Laboratory of Crop Genetic Improvement, National Center of Oil Crop Improvement (Wuhan), College of Plant Science and Technology, Huazhong Agricultural University, Wuhan 430070, People's Republic of China  
e-mail: gexianhong@mail.hzau.edu.cn

D. Gong  
Jingzhou Academy of Agricultural Science, Jingzhou 434007, China

rare in flowers. In this study, the causal genes for the purple/red traits in stems and flowers in two accessions of oilseed rape (DH\_PR and DH\_GC001, respectively) derived from the wide hybridization were fine mapped, and candidate genes were determined by methods combined with bulked segregant analysis (BSA) and RNA-seq analysis. Both traits of purple stem and red flowers were mapped to the locus as *AtPAP2* homologous genes (*BnaPAP2.C6a* and *BnaPAP2.A7b*, respectively) belonging to the R2R3-MYB family. Sequence comparisons of full-length allelic genes revealed several InDels and SNPs in intron 1 as well as exons, and completely different promoter region of *BnaPAP2.C6a* and a 211 bp insertion was identified in the promoter region of *BnaPAP2.A7b* of DH\_GC001. Our results not only contribute to a better understanding of anthocyanin inheritance in *B. napus*, but also provide a useful toolbox for future breeding of cultivars with purple/red traits through the combination of different functional alleles and homologs.

**Keywords** *Brassica napus* · Fine mapping · Flower color · Anthocyanins

C. Cui   
Environment-Friendly Crop Germplasm Innovation and Genetic Improvement Key Laboratory of Sichuan Province, Crop Research Institute, Sichuan Academy of Agricultural Sciences, Chengdu 610066, China  
e-mail: cuicheng005@163.com

## Introduction

Anthocyanins are water-soluble pigments that play a wide range of functions in plants, such as responses to biological and abiotic adversity and the attraction of pollinators and seed dispersal (Zhang et al. 2014). Anthocyanins also benefit humans by lowering the risk of cancer, diabetes, and cardiovascular diseases (Khoo et al. 2017). The biosynthesis of anthocyanins is highly organized and primarily from the phenylpropanoid metabolic pathway of phenylalanine. Many enzymes encoded by structural genes are involved in the biosynthesis of anthocyanins, including chalcone synthase (CHS), chalcone isomerase (CHI), flavanone 3-hydroxylase (F3H), flavonoid 3-O-hydroxylase (F3'H), dihydroflavonol 4-reductase (DFR), anthocyanidin synthase (ANS)/leucoanthocyanidin dioxygenase (LDOX), and anthocyanidin 3-O-glucosyltransferase (UFGT) (Koes et al. 2005; Lepiniec et al. 2006; Petroni and Tonelli 2011; Routaboul et al. 2012; Zhang et al. 2014).

The regulation of anthocyanin biosynthesis usually occurs at the transcriptional level of structural genes by the combined action of R2R3-MYB and R/B-like basic helix-loop-helix (bHLH) transcription factors (TFs), together with WD repeat protein TRANSPARENT TESTA GLABRA1 (TTG1), in a MBW ternary protein complex (Zimmermann et al. 2004; Gonzalez et al. 2008; Dubos et al. 2010; Hichri et al. 2011). In *Arabidopsis*, *MYB75(PAP1)/MYB90 (PAP2) /MYB113/MYB114* were reported as key genes to regulate anthocyanin biosynthesis pathway genes (*DFR* and *LDOX*) in vegetative tissues (Stracke et al. 2007). Overexpression of these genes can significantly improve anthocyanin synthesis in various plants. For example, overexpression of *PAP1* programmed a complete anthocyanin pathway leading to creation of purple tobacco plants (He et al. 2017; Li et al. 2019). The overexpression of the *Raphanus sativus* *RsMYB1* enhances anthocyanin accumulation in flowers of transgenic *Petunia* and their hybrids (Naing et al. 2020). Gained functional mutations, especially those resulting from transposon insertion, usually lead to the upregulation of R2R3-MYB genes and in turn lead to the accumulation of anthocyanin in certain organs and tissues. For example, in *Citrus*, the insertion of retrotransposons adjacent to a gene encoding Ruby, a MYB transcriptional activator of anthocyanin

production, activates gene expression and results in the blood orange phenotype (Butelli et al. 2012).

*Brassica* crops are major oil crops, important vegetables, and forages, including three diploids, *B. rapa* (AA,  $2n=20$ ), *B. oleracea* (CC,  $2n=18$ ), and *B. nigra* (BB,  $2n=16$ ), and three allotetraploids derived from the hybridization between diploids, *B. napus* (AACC,  $2n=38$ ), *B. juncea* (AABB,  $2n=36$ ), and *B. carinata* (BBCC,  $2n=34$ ). *Brassica* shares a common ancestor with *Arabidopsis*, but each of the *Brassica* genomes has undergone a Brassicaceae-lineage-specific whole-genome triplication since their divergence from the *Arabidopsis* lineage (Lysak et al. 2005; Wang et al. 2011; Liu et al. 2014; Parkin et al. 2014; Perumal et al. 2020). Generally, three or more homologous copies of a specific gene in the *Arabidopsis* genome can be found in the *Brassica* genome. Resolving the functional copies responsible for phenotypic variation is a challenge in genetic analysis of *Brassica* species.

Anthocyanin biosynthesis and accumulation, leading to phenotypic variation with purple organ, is a very common phenomenon in *Brassica*. The causal genes underlying the color variation in many vegetable crops have been extensively investigated by gene expression analysis (Zhang et al. 2014; Xie et al. 2014; Song et al. 2018) as well as map-based cloning which indicated that homologous gene of *AtPAP2* plays a key role in regulating the anthocyanin production in *Brassica* (Chiu et al. 2010; Yan et al. 2019; Heng et al. 2020; He et al. 2020; Chen et al. 2022). *B. napus* L. was formed ~7500 years ago by hybridization between the *B. oleracea* and *B. rapa* (Allender and King 2010; 5.Chalhoub et al. 2014). Purple organs are frequently observed in *B. napus* but rarely in petals and the causal genes underlying them remain unknown. In this study, we determined two genes for purple stems and red flowers formation in two accessions of oilseed rape by map-based cloning strategy.

## Materials and methods

### Plant materials

One *B. napus* alien introgression line was obtained from the crosses of (*B. rapa* ssp. *chinensis* L. × *Orychophragmus violaceus*) × *B. napus*, by successive phenotypic selection and cytological observation

(Xu et al. 2019). This line had the same chromosome complement ( $2n=38$ ) as *B. napus* and normal meiotic behavior and good seed set. It was characterized by its purple plant except for yellow petals and was named purple rapeseed (PR). Another *B. napus* accession (GC001) with orange-red flowers was obtained from the high-generation backcross progenies of *B. napus* and the wide hybrids between *B. napus* and *Raphanus sativus* L (Cui, unpublished). Doubled haploid plants of the two accessions were produced by microspore culture and were renamed as DH\_PR and DH\_GC001. Meanwhile, two *B. napus* variety, Zhongshuang 11 (ZS11) and Westar, and one inbred line GL570 with white flowers were used for segregating population development. In the spring of 2020, reciprocal crosses between DH\_PR and ZS11 as well as between DH\_GC001 and GL570 were made, and  $F_1$  hybrids were planted in summer in Hezheng, Gansu province, and then  $F_2$  seeds were obtained and planted in Wuhan in the autumn of 2020 and 2021. In the spring of 2021, the phenotype of each plant was investigated, and young leaves of those 30 plants with extreme phenotype (purple stem vs. green stem and with orange-red and pink flowers vs. yellow and white flowers) in two  $F_2$  populations together with four parent accessions were collected for DNA extraction. In the spring of 2022, the phenotype of each plant was investigated again, and young leaves of those plants with extreme recessive phenotype (green stem or yellow and white flowers) were collected for DNA extraction for fine mapping. For RNA-seq and gene expression analysis, at least five plants of each parent accession were planted in a greenhouse at Huazhong Agricultural University under 16 h light/8 h dark conditions. Young leaves, stems, and petals of newly opened flowers as well as silique walls were collected from at least three plants for RNA extraction. To test the reliability of the markers closely linked to purple stems, another  $F_2$  population was also produced in 2021 using the DH\_PR and Westar as two parents. All rapeseed accessions used in this study are listed in Table S1.

#### DNA extraction, BSA library construction, and Illumina sequencing

The Plant Genomic DNA Isolation Kit (TIANGEN DP320, Beijing) was used to extract total genomic DNA from young leaves, and quantity was checked

using a NanoDrop2000 spectrophotometer (Thermo Scientific, USA). Thirty plants with the same extreme phenotype were combined equally (100 ng per plant) to generate the bulked sample pools. Subsequently, DNA of four pools together with four parents were used to generate paired-end (PE) 150 sequencing libraries according to Illumina library construction protocol and sequenced by Illumina HiSeq™ 3000 platform (Illumina, San Diego, CA, USA). Total genomic DNA of plants with extreme recessive phenotypes in the  $F_2$  population was extracted using the cetyltrimethylammonium bromide (CTAB) method.

#### Bulked segregant analysis

The raw data was used for quality control (Quality Score, Q-value) and processing of the sequencing data by filtering out low-quality and adapter-carrying reads. The clean reads were then mapped to the reference genome of *B. napus* (Darmor-*bzh*) (<http://www.genoscope.cns.fr/brassicapapus/>) (Chalhoub et al. 2014) or Zhongshuang 11 (Song et al. 2020) by the Burrows-Wheeler Aligner (BWA) software (Li and Durbin 2009). GATK toolkit (McKenna et al. 2010) was used to detect and filter SNPs, which were applied to association analysis by calculating the Euclidean distance (ED) between the two pools (Hill et al. 2013). Low-quality SNPs with map quality value < 30, reads depth < 10×, or base quality value < 20 were excluded. After calculating the ED value of each SNP site, a curve chart was drawn about the loess (locally weighted regression) fit of the ED values, in which the threshold was set at median + 3 SD (standard deviation).

#### RNA extraction, RNA-seq, and qRT-PCR analysis

All samples with three biological repeats were collected and immediately stored in liquid nitrogen for RNA extraction. Total RNA was extracted using Eastep Super Total RNA Extract Kit (Promega, Shanghai, China) supplemented with RNase-free DNaseI to remove contaminating DNA according to the manufacturer's instructions. The RNA-seq libraries were constructed according to the user manual (Illumina, <http://www.illumina.com/>) and sequenced by Illumina HiSeq™ 3000 platform to produce 150-bp paired-end reads. Low-quality

reads were removed from the raw reads using the Cutadapt (Martin and Wang 2011) and Trimmomatic (Bolger et al. 2014) software. Clean reads were mapped to the *B. napus* Darmor-*bzh* genome sequence (Chalhoub et al. 2014) using TopHat2 (Kim et al. 2013), and the read counts of each gene were calculated using the HTseq-count function in the HTseq software package (Anders et al. 2015). Gene expression values were calculated in terms of fragments per kilobase of exon model per million mapped reads (FPKM) using Cufflinks (Trapnell et al. 2012), and the differentially expressed genes (DEGs) were identified by the R program DESeq2 (Love et al. 2014). For qRT-PCR analysis, first-strand cDNA was synthesized using a RevertAid First Strand cDNA Synthesis Kit (Thermo, USA). The cDNA was amplified on a CFX96TM Real-time PCR Detection System (Bio-Rad, Germany). The specific quantitative primers for the three transcripts were designed using Primer 5.0; all primer sequences are listed in Table S2. qRT-PCR assays with three biological replicates and three technical repetitions were performed using a Luna Universal qPCR Master Mix (Biolabs, USA). The *Bnaactin3* was used as an internal control for data normalization, and quantitative variation in different replicates was calculated using the delta-delta threshold cycle relative quantification method described previously (Fu et al. 2018).

## Results

### Phenotypic characterization of DH\_PR and DH\_GC001

In the young plant stage, DH\_PR has marked purple young leaves, especially for those heart leaves and petioles compared to ZS11 (Fig. 1A–B), while at the bolting and flowering stage, marked purple color was observed mainly on the stems (Fig. 1C–F). Anatomical observation by hand-free section found that the anthocyanin accumulated mainly in the epidermis and parenchyma cells of DH\_PR (G, H). DH\_GC001 showed orange-red flowers, while GL570 had white flowers, and the hybrids had pink flowers (Fig. 1I–N). It was noticed that the color of the petals of DH\_GC001 faded slowly after the flower opened.

### Fine mapping of genes controlling the purple stem traits in rapeseed

A reciprocal cross between ZS11 and DH\_PR was performed, and all F<sub>1</sub> plants showed purple leaves, stems, and siliques, although the color is lighter than DH\_PR. In the F<sub>2</sub> segregating population, the stem colors could be clearly categorized as purple and green at mature plants stage. Among 370 F<sub>2</sub> individuals, 275 individuals showed purple stems, and 95 individuals showed green stems. The expected Mendelian segregation ratio of 3:1 ( $\chi^2=0.130$ ,  $p>0.05$ ) suggests that the purple stem trait is controlled by a single dominant nuclear gene. The corresponding gene was named the *purple rapeseed stem (PRS)*. Approximately 35.4 GB, 63.2 GB, 28.3 GB, and 22.1 GB of re-sequencing clean data were generated from ZS11, PR, purple stem bulk, and green stem bulk, respectively. A total of 969,463 SNPs and 215,733 InDels were identified between the two bulks using the Darmor-*bzh* as the reference genome. Using the BSA-seq method, the *PRS* gene was finally mapped on the C06 chromosome in the region of 27–32 Mb (Fig. 2A). InDel markers were then designed in the region, and the polymorphism markers were screened. To finely map the *PRS* gene, an F<sub>2</sub>-segregated population of 22,000 individuals was developed, and 5254 plants with extreme green stems were identified. The InDel markers I-015 and I-662 which flanked the candidate region were used to filter recombinant individuals. Using 451 recombinants and the other 10 InDel markers, the *PRS* was finally mapped in an 18.35-kb region between the markers of I-122 and I-126 (Fig. 2B).

### Identification of candidate genes controlling purple stem trait

According to the Darmor-*bzh* reference genome, four coding genes were identified (*BnaC06g27440D*, *BnaC06g27450D*, *BnaC06g27460D*, *BnaC06g27470D*), but no known gene in anthocyanin biosynthesis pathway was found in the candidate region (Fig. 3). However, this genomic region corresponds to 293-kb regions in the *B. napus* (Zhongshuang 11, ZS11) genome (Song et al. 2020) and 284 kb in the NY7 genomes (Zou et al. 2019) (Fig. 4). Two regions contain 34 and 42 predicted protein-coding genes, respectively, and both include three homologous genes of *AtPAP2* (in ZS11 genome: *BnaC06G0328400ZS*, *BnaC06G0328700ZS*, *BnaC06G0329100ZS*). This result



**Fig. 1** Phenotypic characterization of DH\_PR, ZS11, DH\_GC001, and GL570. **A–B** Leaves of DH\_PR (A) and ZS11 (B) at different development stages. **C–D** Part of the plants of DH\_PR (A) and ZS11 (B) at bolting stage. **E–F** Stem of ZS11 (E) and DH\_PR (F). **G–H** Anatomical observation of stems of ZS11 (G) and DH\_PR (H) by hand-free section. **I–N** Inflorescence (I, K, M) and single flower (J, L, N) of GL570, F<sub>1</sub>, and GC\_001, respectively. Bar: 10  $\mu$ m in G and F and 1 cm in others

and DH\_PR (F). **G–H** Anatomical observation of stems of ZS11 (G) and DH\_PR (H) by hand-free section. **I–N** Inflorescence (I, K, M) and single flower (J, L, N) of GL570, F<sub>1</sub>, and GC\_001, respectively. Bar: 10  $\mu$ m in G and F and 1 cm in others

indicated that the genome assembly of the *Darmor-bzh* may be incorrect in the region or that there is structure variation in winter-type rapeseed compared to Chinese semi-winter rapeseed. The ZS11 genome was then used as a reference genome for further analysis. Homologous genes of *AtPAP2* have already been found to respond to the anthocyanin regulation in DH\_PR of leaves (Chen et al. 2020) and purple traits in *B. oleracea* (Yan et al. 2019), *B. rapa* (He et al. 2020), and *B. juncea* (Heng et al. 2020). Thus, these three genes were considered as candidate genes controlling purple phenotype in DH\_PR and renamed as *BnaPAP2.C6a* (*BnaC06G0329100*), *BnaPAP2.C6b* (*BnaC06G0328700*), and *BnaPAP2.C6c* (*BnaC06G0328400*), respectively. RNA-seq analysis of stems indicated that only six genes in the region showed differential expression between two parents (Table S3). *BnaPAP2.C6a* expressed at a significantly higher level in the purple stem of DH\_PR than that in the green stem of ZS11. However, the transcription of *BnaPAP2.C6b* and *BnaPAP2.C6c* was hardly detected both in ZS11 and DH\_PR (Table S3, Fig. 3A). Meanwhile, *BnaPAP2.C6a* expressed at its highest level in the stem, followed

by the silique wall and leaf, but almost silent in the petal. Again, the transcription of the other two genes was hardly detected in all organs of DH\_PR collected here (Fig. 3B). These results further indicated that *BnaPAP2.C6a* is the candidate gene controlling the purple stem formation in DH\_PR.

Whole-length gene cloning revealed that *BnaPAP2.C6a* is 3885 bp (2492 bp promoter and 1393 bp coding region) in DH\_PR and 3918 bp in ZS11 (2506 bp promoter and 1412 bp coding region). Sequence comparison between DH\_PR and ZS11 identified totally different promoter region and several InDels and SNPs in first intron as well as exon 1 and exon 3 (Fig. 4A). Two SNPs in exon 1 and exon 3 led to the change of amino acid from K to E and P to A, respectively. Conserved domain analysis indicated that both variations were in the R2 domain. A PCR marker was designed based on the sequence variation in coding region of *BnaPAP2.C6a*. A new F<sub>2</sub> population with 386 individuals was developed between DH\_PR and Westar, and the phenotype and genotype were investigated. As a result, 286 with purple stems and 100 individuals with green stems were found

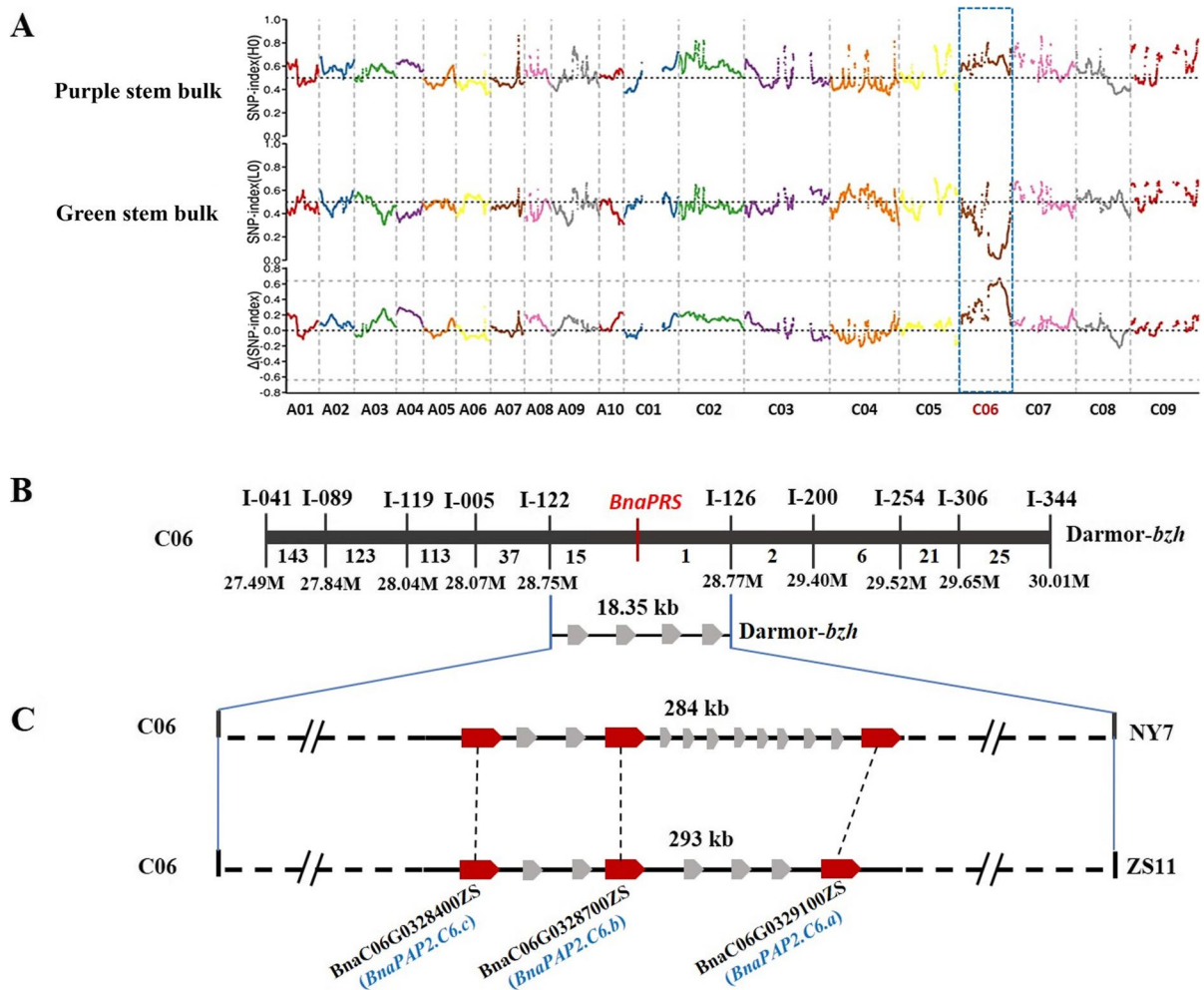


**Fig. 2** Map-based cloning of the *BnaPRS* gene in DH<sub>PR</sub>. **A** The average value of  $\Delta(\text{SNP-index})$  plotted along the nineteen chromosomes (*X*-axis) of *B. napus*. Signals were shown on Chromosome C06. The CIs were simulated with 10,000 times (red,  $p < 0.01$ ; green,  $p < 0.05$ ). **B** Fine mapping of the *BnaPRS* gene between markers I-122 and I-126 on C06. The number below chromosome refers to the number of recom-

binants between two markers. **C** Schematic diagram of predicted genes in the *BnaPRS* locus. The broad arrows mean predicted genes in the 284-Kb and 293-Kb intervals on C06 of NY7 and ZS11, respectively. The *BnaC06G0328400ZS* (*BnaPAP2.C6.c*), *BnaC06G0328700ZS* (*BnaPAP2.C6.b*), and *BnaC06G0329100ZS* (*BnaPAP2.C6.a*) genes were regarded as the candidate genes (red color)

(3:1,  $\chi^2 = 0.17$ ,  $p > 0.05$ ). Genotype detection revealed that gene-specific markers are co-segregated with purple stem plants which included 96 homozygous plants and 190 heterozygous plants (Fig. 4B). Altogether, the *BnaPAP2.C6* gene was considered as the candidate *PRS* gene controlling purple stems in rapeseed.

#### Fine mapping of genes controlling red color flowers

A reciprocal cross between DH<sub>GC001</sub> and GL570 was performed, and all  $F_1$  plants showed pink flowers

(Fig. 1K, L). In the  $F_2$  segregating population, plants have different color flowers from white, light orange, orange, orange-red, pink, red, light yellow, and yellow. In order to exclude the influence of yellow color variation, the flowers of individuals in the  $F_2$  population were divided into two groups: with or without red color. The phenotypic difference is sometimes difficult to distinguish in petals but more obvious in anthers. As a result, among 405 plants of the  $F_2$  population, 312 individuals have flowers with red color, and 93 plants have flowers without red color. The expected Mendelian segregation ratio

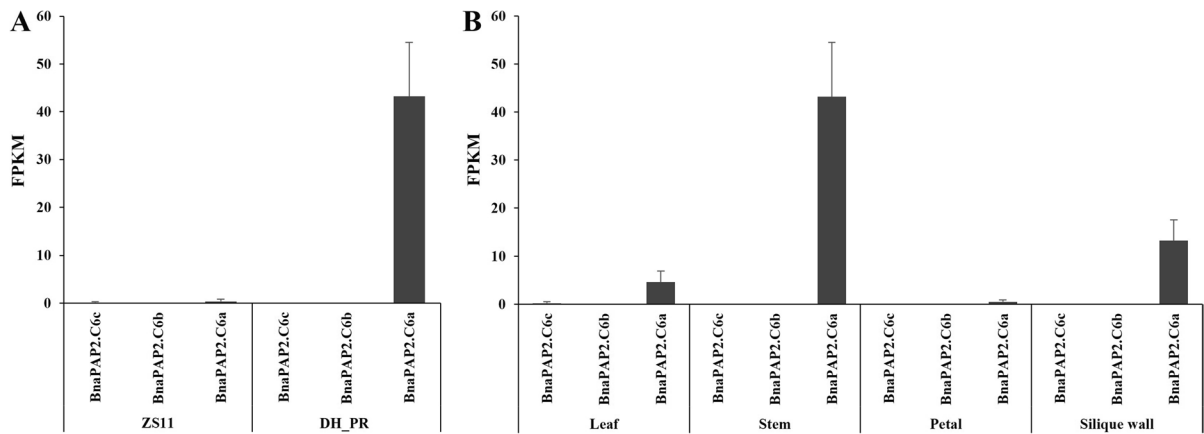
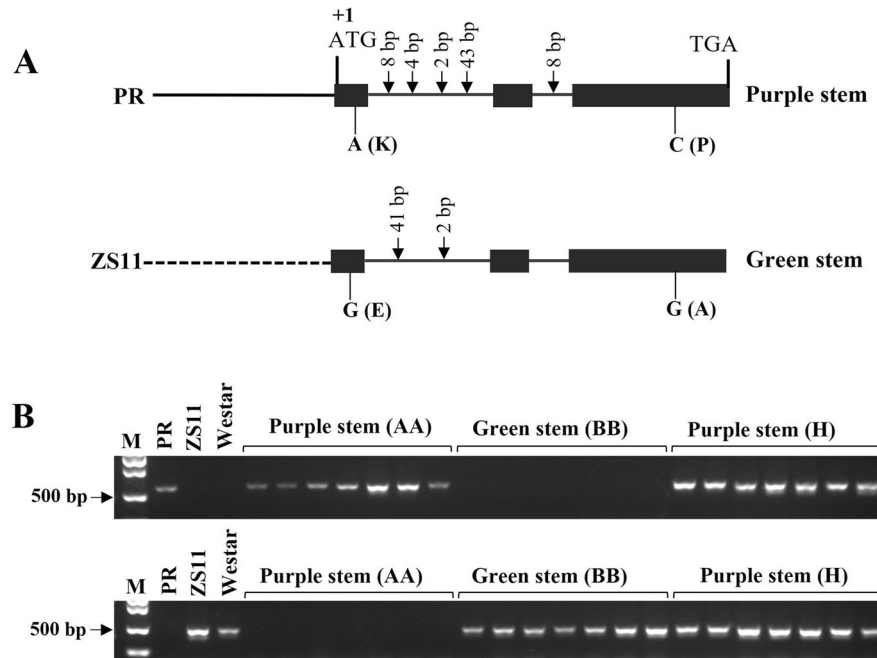


**Fig. 3** Gene expression analysis by RNA-seq analysis of *BnaPAP2.C6a*, *BnaPAP2.C6b*, and *BnaPAP2.C6c*. **A** Expression value of *BnaPAP2.C6a*, *BnaPAP2.C6b*, and *BnaPAP2.C6c* in

stem of DH\_PR and ZS11; **B** expression value of *BnaPAP2.C6a*, *BnaPAP2.C6b*, and *BnaPAP2.C6c* in leaf, stem, petal, and silique wall of DH\_PR

**Fig. 4** Allelic variation of *BnaPAP2.C6a* and co-segregated maker design. **A** Sequence variation of the *BnaPAP2.C6a* alleles. Whole length genes of *BnaPAP2.C6a* of DH\_PR and ZS11 were amplified using primer combination for gene coding region (PAP2.C06.gF/PAP2.C06.gR) and promoter region (PAP2.C06.PF/PAP2.C06.PR). The solid line and dotted line represent that the promoter sequence of the two alleles is completely different. **B** Confirmation of co-segregated maker (ZS11.PAP2.C6.F/ZS11.PAP2.C6.R; PR.PAP2.C6.F/PR.PAP2.C6.R) in  $F_2$  population with 386 individuals derived from DH\_PR  $\times$  Westar



of 3:1 ( $\chi^2=0.954$ ,  $p>0.05$ ) suggests that the red color in flowers is controlled by a single dominant nuclear gene, named the *red rapeseed flower* (*RRF*).

In the  $F_2$  population, 30 plants that have extreme red flowers (orange-red and red) and other 30 plants have extreme yellow and white flowers to produce the bulk pool. Approximately, 38.7 GB, 32.9 GB, 30.6 GB, and 28.3 GB of re-sequencing clean data were generated from DH\_GC001, GL570, bulk of

red flowers, and bulk of flowers without red color, respectively. A total of 1,776,654 SNPs and 597,020 InDels were identified between the two bulks using ZS11 as the reference genome. Using the BSA-seq method, the *RRF* gene was mapped on the A07 chromosome in the region of 23.6–30 Mb (Fig. 5A). InDel markers were then designed in the region, and the polymorphism markers were screened. To finely map the *RRF* gene, an  $F_2$ -segregated population of

5531 individuals was developed, and 1332 extreme plants with white or yellow flowers that have no red color in petals and anthers were identified. 155 InDel markers were designed and used to narrow the target region. Finally, using 454 recombinants and the other 7 InDel markers, the *RRF* gene was finally mapped to a 219.81-kb region between the markers I-80 and I-145. Interestingly, the InDel marker, I-142 was found co-segregated with the purple trait in this segregated population (Fig. 5B).

#### Identification of candidate genes controlling red flowers

According to the reference genomes of ZS11, there are 113 predicted protein-coding genes within the 219.81-kb region (Fig. 5C; Table S4). However, according to the function annotations, only two *AtPAP2* homologous genes *BnaA07G02869000ZS* and *BnaA07G0287000ZS* involved in anthocyanin biosynthesis. Thus, these two genes were considered as candidate genes controlling orange red color flowers in *B. napus* and renamed as *BnaPAP2.A7a* (*BnaA07G02869000ZS*) and *BnaPAP2.A7b* (*BnaA07G0287000ZS*), respectively. To further confirm the genes, RNA-seq analysis was performed using the total RNA extracted from newly opened flower petals of DH\_GC001 and GL570. As a result, among 113 genes within the target region, only three genes show the significantly different expression value between two parents, and only *BnaPAP2.A7b* were significantly upregulated in orange red flowers (Fig. 6A; Table S4). RT-PCR analysis by two primer pairs also confirmed that only *BnaPAP2.A7b* was expressed in petals of DH\_GC001 (Fig. 6B). Gene cloning and allelic sequence comparison indicated that the full length of *BnaPAP2.A7b* in DH\_GC001 is 3557 bp, including the 1665 bp coding region, and is 3345 bp in GL570, including the 1665 bp coding region. There is an extra 211bp insertion in the promoter region at -184 bp of DH\_GC001 (Figure S1A), and no other allelic variation was found. Interestingly, the InDel marker I-142 covered the inserted fragment and exactly co-segregated with the red flower phenotype in the F<sub>2</sub> population (Figure S1B).

#### Discussion

Appearance colors due to anthocyanin accumulation are an important character for commodity as well as

nutritional values in vegetables such as *B. rapa* and *B. oleracea*. Recently, the demand for colored flowers in rapeseed has also prompted researchers to pay more attention to color traits. In this study, we successfully fine mapped two genes controlling pigment accumulation in stems and flowers of rapeseed, respectively, by BSA method which has been widely used in gene mapping of quality traits in *Brassica* crops (Huang et al. 2019; Heng et al. 2020).

*B. napus* usually has yellow flowers, and a few are white flowers. It is already known that the yellow color of the rapeseed flowers is due to the accumulation of carotenoids, while white flowers are formed by a dominant gene for carotenoid degradation (Zhang et al. 2014). Studies have also shown that the appearance of red to purple color in petals of species in Brassicaceae is mainly due to the accumulation of anthocyanins, especially cyanidin (Chen et al. 2018; Fu et al. 2018). While the white flower is dominant to the yellow flower and the red flower is incomplete dominant to the white flower, red and yellow flowers are co-dominant. In order to map the gene controlling red petals as well as to select new accession with colorful flowers, the inbred line GL570 with white flowers but not the inbred line with yellow flowers was chosen as one parent to develop the F<sub>2</sub> population with *B. napus* accession (GC001) with orange red. F<sub>1</sub> plants have petals with a white background, but a few anthocyanins finally showed the pink color. Individuals in such F<sub>2</sub> population presented more colorful patterns than those in F<sub>2</sub> population derived from the hybridization between inbred lines with yellow flowers and GC001.

Because the biosynthesis pathway of the anthocyanin is well known in *Arabidopsis*, two candidate genes (*BnaPAP2.C6a* and *BnaPAP2.A7b*) were determined according to the gene expression analysis as well as allelic sequence comparison. Similarly, *AtPAP2* homologous genes have already found responses to purple color formation in *B. rapa* (He et al. 2020), *B. oleracea* (Chiu et al. 2010; Yan et al. 2019), and *B. juncea* (Heng et al. 2020) as well as in *B. napus* (Chen et al. 2020). Both genes showed significantly increased/activated transcription levels in stems and petals of DH\_PR and DH\_GC001, respectively. Compared to ZS11, despite several SNPs in the exon and intron of *BnaPAP2.C6a*, a completely different promoter region in DH\_PR was identified. Two SNPs in exon 1 and exon 3 of DH\_PR led to amino acid change



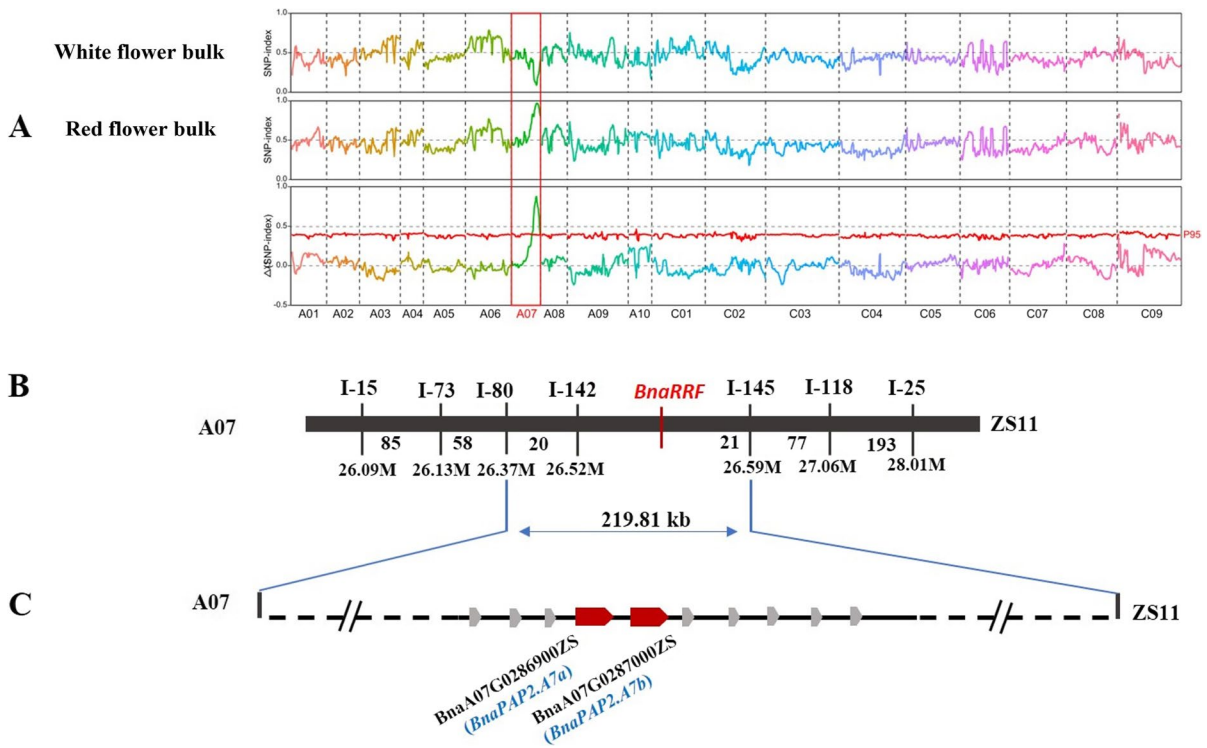
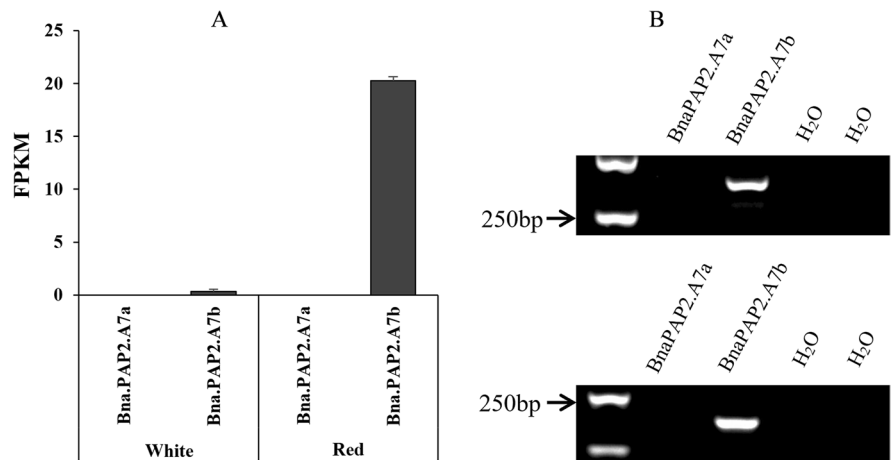


**Fig. 5** Map-based cloning of the *RRF* gene in GC\_001. **A** The average value of  $\Delta$ (SNP-index) plotted along the nineteen chromosomes (*X*-axis) of *B. napus*. Signals were shown on chromosome A07. The CIs were simulated with 10,000 times (red,  $p < 0.01$ ; green,  $p < 0.05$ ). **B** Fine mapping of the *RRF* gene between markers I-180 and I-145 on A07. The number

on the left refers to the recombinants between two markers. **C** Schematic diagram of predicted genes in the *BnaRRF* locus. The broad arrows mean predicted genes in the 219.81-Kb intervals on A07. The *BnaA07G0286900ZS (BnaPAP2.A7a)* and *BnaA07G0287000ZS (BnaPAP2.A7b)* genes were regarded as the candidate genes (red color)

**Fig. 6** Gene expression analysis of *BnaPAP2.A7a* and *BnaPAP2.A7b* in petals. **A** Expression value revealed by RNA-seq analysis of *BnaPAP2.A7a* and *BnaPAP2.A7b* in white and red flowers of GL570 and DH\_GC001, respectively. **B** Semi-quantitative RT-PCR analysis of *BnaPAP2.A7a* and *BnaPAP2.A7b* in red petals of DH\_GC001 by two primers pairs for each gene



which was located in the conserved R2 domain. But *BnaPAP2.C6a* of ZS11 can regulate anthocyanin production in Westar when derived by the 35S promoter (Ge et al., unpublished). These results indicated that

the different promoter of *BnaPAP2.C6a* might promote its expression in DH\_PR and led to purple color formation. However, at present, we do not know where this promoter comes from. No sequence variation in exon

and intron were found of *BnaPAP2.A7b* between DH\_GC001 and GL570, but a 211 bp insertion was found in the promoter region of the allele of DH\_GC001. Interestingly, rapeseed lacks red petals in natural variation, and the red-petaled rapeseed used in this study comes from the distant hybridization of rapeseed and radish. The 211 bp insertion in the promoter region of this gene might be induced by wide hybridization.

The activation of the R2R3-MYB regulating anthocyanin biosynthesis is often caused by insertion of a transposon, as found for example in blood orange (Butelli et al. 2012), tea (Sun et al. 2016), and *Phalaenopsis* orchids (Hsu et al. 2019). Similarly, cis-regulatory variation activates the R2R3 MYB genes and expands the color palette of the Brassicaceae (Fattorini and Ó'Maoláidigh 2022). In *B. oleracea* var. *botrytis*, it was found that *BoMYB2*, one homologous gene of *AtPAP2* in *B. oleracea*, is the key gene giving the striking mutant phenotype of intense purple color in curds and a few other tissues, and a Harbinger DNA transposon insertion in the upstream regulatory region of *BoMYB2* is responsible for the upregulation of the gene (Chiu et al. 2010). *BoMYB2* was also identified as the key gene leading to purple traits in kale, kohlrabi, and cabbage (Yan et al. 2019). However, instead of the insertion of Harbinger transposon, a 7606-bp CACTA-like transposon was found in promoter region of *BoMYB2* in purple kale (*B. oleracea* var. *albobolabra*) and kohlrabi (*B. oleracea* var. *gongylodes*), and the activation of the *BoMYB2* gene in purple cabbage (*B. oleracea* var. *capitata*) was caused by point mutation and/or 1-bp insertion in its promoter region (Yan et al. 2019). In *B. rapa* and *B. juncea*, the orthologous genes of *BrMYB2*, located on chromosome A07 was found to control the dominant purple-head trait of Chinese cabbage and purple leaves in *B. juncea* and the activation of the *BrMYB2* under the control of the short intron 1 (He et al. 2020). In *B. napus*, it was revealed that *BnaPAP2.A7b* is the key gene regulating anthocyanin accumulation in leaves of PR. SNP variations in its promoter region led to the activation of its expression and leading to the purple color formation in leaves (Chen et al. 2020). Recently, map-based cloning also revealed that *BnaPAP2.A07* is responsible for anthocyanin-based flower color and indicated that two insertions (412 bp and 210 bp) in the promoter region are responsible for the transcriptional activation of the gene in flowers (Ye et al. 2022). Altogether, it is speculated that the

sequence variations in the promoter region of *BnaPAP2.C6a* and an insertion in the promoter region of *BnaPAP2.A7b* might be the key reasons leading to the transcription upregulation/activation and leading to pigment accumulation in different organs in *B. napus*.

In polyploids, duplicated genes resulting from whole-genome duplication usually experience three fates: silenced, new functionalization, or sub-functionalization, in which duplicated copies execute the same function but in different parts of the plants (Moore and Purugganan 2005; Roulin et al. 2013). Here, two genes for anthocyanin accumulation in stems and flowers of rapeseed were identified by the map-based cloning method. While sequence variation in the promoter regions of *BnaPAP2.C6a* lead to the activation of the gene in stems, an insertion in the promoter region of *BnaPAP2.A7b* is responsible for the activation of the gene in flowers. The results indicated that these homologous genes may experience sub-functional divergence and expand the color palette of the oilseed rape.

**Acknowledgements** We thank Dr. Bo Wang and Mr. Chaocheng Guo for their help in BSA and RNA-seq analysis.

**Author contribution** XG, JW, and CC conceived and designed the experiments. DC, QJ, YL, JP, YT, YE, LX, JQ, and XC performed the experiments. DC, TY, DG, and XG analyzed the data. DC, XG, and ZL wrote the manuscript.

**Funding** This work was mainly supported by the National Key Research and Development Program of China (2021YFD1600500); the National Natural Science Foundation of China (32160454); and the Natural Science Foundation of Jiangxi Province (20212BAB215002).

**Data availability** Next-generation sequencing data was submitted to NCBI under PRJAN855492. Full-length genes sequence of *BnaPAP2.A7b* and *BnaPAP2.C6a* were also submitted to NCBI under number: BankIt2599524.

**Declarations**

**Conflict of interest** The authors declare no competing interests.

## References

- Allender CJ, King GJ (2010) Origins of the amphiploid species *Brassica napus* L. investigated by chloroplast and nuclear molecular markers. *BMC Plant Biol* 10:54
- Anders S, Pyl PT, Huber W (2015) HTSeq—a Python framework to work with high-throughput sequencing data. *Bioinformatics* 31(2):166–169. <https://doi.org/10.1093/bioinformatics/btu638>

- Bolger AM, Lohse M, Usadel B (2014) Trimmomatic: a flexible trimmer for Illumina sequence data. *Bioinformatics* 30(15):2114–2120. <https://doi.org/10.1093/bioinformatics/btu170>
- Butelli E, Licciardello C, Zhang Y, Liu J, Mackay S, Bailey P, Reforgiato-Recupero G, Martin C (2012) Retrotransposons control fruit-specific, cold-dependent accumulation of anthocyanins in blood oranges. *Plant Cell* 24(3):1242–1255. <https://doi.org/10.1105/tpc.111.095232>
- Chalhoub B, Denoeud F, Liu S, Parkin IA, Tang H, Wang X, Chiquet J, Belcram H, Tong C, Samans B, Corréa M, Da Silva C, Just J, Falentin C, Koh CS, Le Clainche I, Bernard M, Bento P, Noel B, Labadie K, Alberti A, Charles M, Arnaud D, Guo H, Daviaud C, Alamery S, Jabbari K, Zhao M, Edger PP, Chelaifa H, Tack D, Lassalle G, Messtiri I, Schnel N, Le Paslier MC, Fan G, Renault V, Bayer PE, Golicz AA, Manoli S, Lee TH, Thi VH, Chalabi S, Hu Q, Fan C, Tollenaere R, Lu Y, Battail C, Shen J, Sidebottom CH, Wang X, Canaguier A, Chauveau A, Bérard A, Deniot G, Guan M, Liu Z, Sun F, Lim YP, Lyons E, Town CD, Bancroft I, Wang X, Meng J, Ma J, Pires JC, King GJ, Brunel D, Delourme R, Renard M, Aury JM, Adams KL, Batley J, Snowdon RJ, Tost J, Edwards D, Zhou Y, Hua W, Sharpe AG, Paterson AH, Guan C, Wincker P (2014) Plant genetics. Early allopolyploid evolution in the post-Neolithic *Brassica napus* oilseed genome. *Science* 345(6199):950–3. <https://doi.org/10.1126/science.1253435>
- Chen D, Liu Y, Yin S, Qiu J, Jin Q, King GJ, Wang J, Ge X, Li Z (2020) Alternatively spliced BnaPAP2A7 isoforms play opposing roles in anthocyanin biosynthesis of *Brassica napus* L. *Front Plant Sci* 11:983. <https://doi.org/10.3389/fpls.2020.00983>
- Chen D, Chen H, Dai G, Zhang H, Liu Y, Shen W, Zhu B, Cui C, Tan C (2022) Genome-wide identification of R2R3-MYB gene family and association with anthocyanin biosynthesis in *Brassica* species. *BMC Genomics* 23(1):441. <https://doi.org/10.1186/s12864-022-08666-7>
- Chen DZ, Liu Y, Pan Q, Li FF, Zhang QH, Ge XH, Li Zaiyun (2018) De novo transcriptome assembly, gene expressions and metabolites for flower color variation of two garden species in Brassicaceae. *Scientia Horticulturae*: 592–602. <https://doi.org/10.1016/j.scienta.2018.06.057>
- Chiu LW, Zhou X, Burke S, Wu X, Prior RL, Li L (2010) The purple cauliflower arises from activation of a MYB transcription factor. *Plant Physiol* 154(3):1470–1480. <https://doi.org/10.1104/pp.110.164160>
- Dubos C, Stracke R, Grotewold E, Weisshaar B, Martin C, Lepiniec L (2010) MYB transcription factors in Arabidopsis. *Trends Plant Sci* 15(10):573–581. <https://doi.org/10.1016/j.tplants.2010.06.005>
- Fattorini R, Ó'Maoiléidigh DS (2022) Cis-regulatory variation expands the colour palette of the Brassicaceae. *J Exp Bot* 73(19):6511–6515. <https://doi.org/10.1093/jxb/erac366>. PMID:36322901;PMCID:PMC9629846
- Fu W, Chen D, Pan Q, Li F, Zhao Z, Ge X, Li Z (2018) Production of red-flowered oilseed rape via the ectopic expression of *Orychophragmus violaceus* OvPAP2. *Plant Biotechnol J* 16(2):367–380. <https://doi.org/10.1111/pbi.12777>
- Gonzalez A, Zhao M, Leavitt JM, Lloyd AM (2008) Regulation of the anthocyanin biosynthetic pathway by the TTG1/bHLH/Myb transcriptional complex in Arabidopsis seedlings. *Plant J* 53(5):814–827. <https://doi.org/10.1111/j.1365-313X.2007.03373.x>
- He X, Li Y, Lawson D, Xie D-Y (2017) Metabolic engineering of anthocyanins in dark tobacco varieties. *Physiol Plant* 159:2–12
- He Q, Wu J, Xue Y, Zhao W, Li R, Zhang L (2020) The novel gene BrMYB2, located on chromosome A07, with a short intron 1 controls the purple-head trait of Chinese cabbage (*Brassica rapa* L.). *Hortic Res* 7:97. <https://doi.org/10.1038/s41438-020-0319-z>
- Heng SP, Huang H, Cui MD, Liu MF, Lv Q, Hu PY, Ren SJ, Li X, Fu TD, Wan ZJ (2020) Rapid identification of the BjRCO gene associated with lobed leaves in *Brassica juncea* via bulked segregant RNA-seq. *Mol Breeding* 40:42. <https://doi.org/10.1007/s11032-020-01119-7>
- Heng S, Cheng Q, Zhang T, Liu X, Huang H, Yao P, Liu Z, Wan Z, Fu T (2020) Fine-mapping of the BjPur gene for purple leaf color in *Brassica juncea*. *Theor Appl Genet* 133(11):2989–3000. <https://doi.org/10.1007/s00122-020-03634-9>
- Hichri I, Barrieu F, Bogs J, Kappel C, Delrot S, Lauvergeat V (2011) Recent advances in the transcriptional regulation of the flavonoid biosynthetic pathway. *J Exp Bot* 62(8):2465–2483. <https://doi.org/10.1093/jxb/erq442>
- Hill JT, Demarest BL, Bisgrove BW, Gorski B, Su YC, Yost HJ (2013) MMAPP: mutation mapping analysis pipeline for pooled RNA-seq. *Genome Res* 23(4):687–697. <https://doi.org/10.1101/gr.146936.112>
- Hsu CC, Su CJ, Jeng MF, Chen WH, Chen HH (2019) A HORT1 retrotransposon insertion in the PeMYB11 promoter causes Harlequin/black flowers in *Phalaenopsis* orchids. *Plant Physiol* 180(3):1535–1548. <https://doi.org/10.1104/pp.19.00205>
- Huang Z, Peng G, Gossen BD, Yu F (2019) Fine mapping of a clubroot resistance gene from turnip using SNP markers identified from bulked segregant RNA-Seq. *Mol Breeding* 39:131. <https://doi.org/10.1007/s11032-019-1038-8>
- Khoo HE, Azlan A, Tang ST, Lim SM (2017) Anthocyanidins and anthocyanins: colored pigments as food, pharmaceutical ingredients, and the potential health benefits. *Food Nutr Res* 61:1. <https://doi.org/10.1080/16546628.2017.1361779>
- Kim D, Perteau G, Trapnell C, Pimentel H, Kelley R, Salzberg SL (2013) TopHat2: accurate alignment of transcriptomes in the presence of insertions, deletions and gene fusions. *Genome Biol* 14(4):R36. <https://doi.org/10.1186/gb-2013-14-4-r36>
- Koes R, Verweij W, Quattrocchio F (2005) Flavonoids: a colorful model for the regulation and evolution of biochemical pathways. *Trends Plant Sci* 10(5):236–242. <https://doi.org/10.1016/j.tplants.2005.03.002>
- Lepiniec L, Debeaujon I, Routaboul JM, Baudry A, Pourcel L, Nesi N, Caboche M (2006) Genetics and biochemistry of seed flavonoids. *Annu Rev Plant Biol* 57:405–430. <https://doi.org/10.1146/annurev.arplant.57.032905.105252>
- Li H, Durbin R (2009) Fast and accurate short read alignment with Burrows-Wheeler transform. *Bioinformatics* 25(14):1754–1760. <https://doi.org/10.1093/bioinformatics/btp324>
- Li G, Ji XM, Xi J, Xie DY, Su XH (2019) Creation of elite growth and development features in PAPI-programmed red *Nicotiana tabacum* Xanthi via overexpression of synthetic geranyl pyrophosphate synthase genes. *Mol Breeding* 39:63. <https://doi.org/10.1007/s11032-019-0968-5>

- Liu S, Liu Y, Yang X, Tong C, Edwards D, Parkin IA, Zhao M, Ma J, Yu J, Huang S, Wang X, Wang J, Lu K, Fang Z, Bancroft I, Yang TJ, Hu Q, Wang X, Yue Z, Li H, Yang L, Wu J, Zhou Q, Wang W, King GJ, Pires JC, Lu C, Wu Z, Sampath P, Wang Z, Guo H, Pan S, Yang L, Min J, Zhang D, Jin D, Li W, Belcram H, Tu J, Guan M, Qi C, Du D, Li J, Jiang L, Batley J, Sharpe AG, Park BS, Ruperao P, Cheng F, Waminal NE, Huang Y, Dong C, Wang L, Li J, Hu Z, Zhuang M, Huang Y, Huang J, Shi J, Mei D, Liu J, Lee TH, Wang J, Jin H, Li Z, Li X, Zhang J, Xiao L, Zhou Y, Liu Z, Liu X, Qin R, Tang X, Liu W, Wang Y, Zhang Y, Lee J, Kim HH, Denoed F, Xu X, Liang X, Hua W, Wang X, Wang J, Chalhoub B, Paterson AH (2014) The Brassica oleracea genome reveals the asymmetrical evolution of polyploid genomes. *Nat Commun* 23(5):3930. <https://doi.org/10.1038/ncomms4930>
- Love MI, Huber W, Anders S (2014) Moderated estimation of fold change and dispersion for RNA-seq data with DESeq2. *Genome Biol* 15:550. <https://doi.org/10.1186/s13059-014-0550-8>
- Lysak MA, Koch MA, Pecinka A, Schubert I (2005) Chromosome triplication found across the tribe Brassiceae. *Genome Res* 15(4):516–525. <https://doi.org/10.1101/gr.3531105>
- Martin JA, Wang Z (2011) Next-generation transcriptome assembly. *Nat Rev Genet* 12(10):671–682. <https://doi.org/10.1038/nrg3068>
- McKenna A, Hanna M, Banks E, Sivachenko A, Cibulskis K, Kernytzky A, Garimella K, Altshuler D, Gabriel S, Daly M, DePristo MA (2010) The Genome Analysis Toolkit: a MapReduce framework for analyzing next-generation DNA sequencing data. *Genome Res* 20(9):1297–1303. <https://doi.org/10.1101/gr.107524.110>
- Moore RC, Purugganan MD (2005) The evolutionary dynamics of plant duplicate genes. *Curr Opin Plant Biol* 8(2):122–128. <https://doi.org/10.1016/j.pbi.2004.12.001>
- Naing AH, Kang HH, Jeong HY, Soe MT, Xu JP, Kim CK (2020) Overexpression of the *Raphanus sativus* RsMYB1 using the flower-specific promoter (InMYB1) enhances anthocyanin accumulation in flowers of transgenic *Petunia* and their hybrids. *Mol Breeding* 40:97. <https://doi.org/10.1007/s11032-020-01176-y>
- Parkin IA, Koh C, Tang H, Robinson SJ, Kagale S, Clarke WE, Town CD, Nixon J, Krishnakumar V, Bidwell SL, Denoed F, Belcram H, Links MG, Just J, Clarke C, Bender T, Huebert T, Mason AS, Pires JC, Barker G, Moore J, Walley PG, Manoli S, Batley J, Edwards D, Nelson MN, Wang X, Paterson AH, King G, Bancroft I, Chalhoub B, Sharpe AG (2014) Transcriptome and methylome profiling reveals relics of genome dominance in the mesopolyploid Brassica oleracea. *Genome Biol* 15(6):R77. <https://doi.org/10.1186/gb-2014-15-6-r77>
- Perumal S, Koh CS, Jin L, Buchwaldt M, Higgins EE, Zheng C, Sankoff D, Robinson SJ, Kagale S, Navabi ZK, Tang L, Horner KN, He Z, Bancroft I, Chalhoub B, Sharpe AG, Parkin IAP (2020) A high-contiguity Brassica nigra genome localizes active centromeres and defines the ancestral Brassica genome. *Nat Plants* 6(8):929–941. <https://doi.org/10.1038/s41477-020-0735-y>
- Petroni K, Tonelli C (2011) Recent advances on the regulation of anthocyanin synthesis in reproductive organs. *Plant Sci* 181(3):219–229. <https://doi.org/10.1016/j.plantsci.2011.05.009>
- Roulin A, Auer PL, Libault M, Schlueter J, Farmer A, May G, Stacey G, Doerge RW, Jackson SA (2013) The fate of duplicated genes in a polyploid plant genome. *Plant J* 73(1):143–153. <https://doi.org/10.1111/tpj.12026>
- Routaboul JM, Dubos C, Beck G, Marquis C, Bidzinski P, Loudet O, Lepiniec L (2012) Metabolite profiling and quantitative genetics of natural variation for flavonoids in Arabidopsis. *J Exp Bot* 63(10):3749–3764. <https://doi.org/10.1093/jxb/ers067>
- Song H, Yi H, Lee M, Han CT, Lee J, Kim H, Park JI, Nou IS, Kim SJ, Hur Y (2018) Purple Brassica oleracea var. capitata F rubra. is due to the loss of BoMYB2L–1 expression. *BMC Plant Biol* 18(1):82. <https://doi.org/10.1186/s12870-018-1290-9>
- Song JM, Guan Z, Hu J, Guo C, Yang Z, Wang S, Liu D, Wang B, Lu S, Zhou R, Xie WZ, Cheng Y, Zhang Y, Liu K, Yang QY, Chen LL, Guo L (2020) Eight high-quality genomes reveal pan-genome architecture and ecotype differentiation of Brassica napus. *Nat Plants* 6(1):34–45. <https://doi.org/10.1038/s41477-019-0577-7>
- Stracke R, Ishihara H, Hup G, Barsch A, Mehrrens F, Niehaus K, Weisshaar B (2007) Differential regulation of closely related R2R3-MYB transcription factors controls flavonol accumulation in different parts of the Arabidopsis thaliana seedling. *Plant J* 50(4):660–677. <https://doi.org/10.1111/j.1365-3113X.2007.03078.x>
- Sun B, Zhu Z, Cao P, Chen H, Chen C, Zhou X, Mao Y, Lei J, Jiang Y, Meng W, Wang Y, Liu S (2016) Purple foliage coloration in tea (*Camellia sinensis* L.) arises from activation of the R2R3-MYB transcription factor CsAN1. *Sci Rep* 6:32534. <https://doi.org/10.1038/srep32534>
- Trapnell C, Roberts A, Goff L, Pertea G, Kim D, Kelley DR, Pimentel H, Salzberg SL, Rinn JL, Pachter L (2012) Differential gene and transcript expression analysis of RNA-seq experiments with TopHat and Cufflinks. *Nat Protoc* 7(3):562–578. <https://doi.org/10.1038/nprot.2012.016>
- Wang X, Wang H, Wang J, Sun R, Wu J, Liu S, Bai Y, Mun JH, Bancroft I, Cheng F, Huang S, Li X, Hua W, Wang J, Wang X, Freeling M, Pires JC, Paterson AH, Chalhoub B, Wang B, Hayward A, Sharpe AG, Park BS, Weisshaar B, Liu B, Li B, Liu B, Tong C, Song C, Duran C, Peng C, Geng C, Koh C, Lin C, Edwards D, Mu D, Shen D, Soumpourou E, Li F, Fraser F, Conant G, Lassalle G, King GJ, Bonnema G, Tang H, Wang H, Belcram H, Zhou H, Hirakawa H, Abe H, Guo H, Wang H, Jin H, Parkin IA, Batley J, Kim JS, Just J, Li J, Xu J, Deng J, Kim JA, Li J, Yu J, Meng J, Wang J, Min J, Poulain J, Wang J, Hatakeyama K, Wu K, Wang L, Fang L, Trick M, Links MG, Zhao M, Jin M, Ramchiary N, Drou N, Berkman PJ, Cai Q, Huang Q, Li R, Tabata S, Cheng S, Zhang S, Zhang S, Huang S, Sato S, Sun S, Kwon SJ, Choi SR, Lee TH, Fan W, Zhao X, Tan X, Xu X, Wang Y, Qiu Y, Yin Y, Li Y, Du Y, Liao Y, Lim Y, Narusaka Y, Wang Y, Wang Z, Li Z, Wang Z, Xiong Z, Zhang Z, Brassica rapa Genome Sequencing Consortium (2011) The genome of the mesopolyploid crop species Brassica rapa. *Nat Genet* 43(10):1035–9. <https://doi.org/10.1038/ng.919>
- Wang Y, Tang H, Debarry JD, Tan X, Li J, Wang X, Lee TH, Jin H, Marler B, Guo H, Kissinger JC, Paterson AH (2012) MScanX: a toolkit for detection and evolutionary analysis of gene synteny and collinearity. *Nucleic Acids Res* 40(7):e49. <https://doi.org/10.1093/nar/gkr1293>

- Xie Q, Hu Z, Zhang Y, Tian S, Wang Z, Zhao Z, Yang Y, Chen G (2014) Accumulation and molecular regulation of anthocyanin in purple tumorous stem mustard (*Brassica juncea* var. *tumida* Tsen et Lee). *J Agric Food Chem* 62(31):7813–21. <https://doi.org/10.1021/jf501790a>
- Xu C, Huang Q, Ge X, Li Z (2019) Phenotypic, cytogenetic, and molecular marker analysis of *Brassica napus* introgressants derived from an intergeneric hybridization with *Orychophragmus*. *PLoS One* 14(1):e0210518. <https://doi.org/10.1371/journal.pone.0210518>
- Yan C, An G, Zhu T, Zhang W, Zhang L, Peng L, Chen J, Kuang H (2019) Independent activation of the BoMYB2 gene leading to purple traits in *Brassica oleracea*. *Theor Appl Genet* 132(4):895–906. <https://doi.org/10.1007/s00122-018-3245-9>
- Ye S, Hua S, Ma T, Ma X, Chen Y, Wu L, Zhao L, Yi B, Ma C, Tu J, Shen J, Fu T, Wen J (2022) Genetic and multi-omics analysis reveal BnaA07.PAP2In-184–317 as the key gene conferring anthocyanin-based color in *Brassica napus* flowers. *J Exp Bot:erac312*. <https://doi.org/10.1093/jxb/erac312>
- Zhang Y, Butelli E, Martin C (2014) Engineering anthocyanin biosynthesis in plants. *Curr Opin Plant Biol* 19:81–90. <https://doi.org/10.1016/j.pbi.2014.05.011>
- Zhang B, Liu C, Wang Y, Yao X, Wang F, Wu J, King GJ, Liu K (2015) Disruption of a CAROTENOID CLEAVAGE DIOXYGENASE 4 gene converts flower colour from white to yellow in *Brassica* species. *New Phytol* 206(4):1513–1526. <https://doi.org/10.1111/nph.13335>
- Zimmermann IM, Heim MA, Weisshaar B, Uhrig JF (2004) Comprehensive identification of *Arabidopsis thaliana* MYB transcription factors interacting with R/B-like BHLH proteins. *Plant J* 40(1):22–34. <https://doi.org/10.1111/j.1365-3113X.2004.02183.x>
- Zou J, Mao L, Qiu J, Wang M, Jia L, Wu D, He Z, Chen M, Shen Y, Shen E, Huang Y, Li R, Hu D, Shi L, Wang K, Zhu Q, Ye C, Bancroft I, King GJ, Meng J, Fan L (2019) Genome-wide selection footprints and deleterious variations in young Asian allotetraploid rapeseed. *Plant Biotechnol J* 17(10):1998–2010. <https://doi.org/10.1111/pbi.13115>

**Publisher's note** Springer Nature remains neutral with regard to jurisdictional claims in published maps and institutional affiliations.

Springer Nature or its licensor (e.g. a society or other partner) holds exclusive rights to this article under a publishing agreement with the author(s) or other rightsholder(s); author self-archiving of the accepted manuscript version of this article is solely governed by the terms of such publishing agreement and applicable law.